Title: Evaluation of preservation protocols for oxygen-sensitive minerals within laminated aquatic sediments

Authors: *[1]Ledesma, Gabrielle, *[1]Islam, Raisa, and [1]Elizabeth D. Swanner

[1] Department of Geological and Atmospheric Sciences, Iowa State University, Ames, Iowa, USA

(*these authors contributed equally to this work)

This paper is a non-peer reviewed preprint submitted to EarthArXiv. The preprint has also been submitted to *Limnology and Oceanography Methods*.

Keywords: sediment, preservation, redox, minerals, embedding, iron, manganese, sulfur

Twitter Handles:

GL – @LedesmaGabbie

RI - @raisa_islam9

EDS - @betsyswanner

Abstract

Laminated sediments can record seasonal changes in sedimentation of material from anoxic waters, including minerals of the redox-sensitive elements Fe, Mn, and S that form under varying oxygen levels, mineral saturation conditions, and from microbial metabolism. However, preserving both the oxygen-sensitive minerals for identification is challenging when preservation of the spatial arrangement of laminae is also required. In this study, we compare methods for embedding sedimentary materials from anoxic waters and sediments from Brownie Lake, Minnesota, USA for analysis of the redox speciation for Fe, Mn, and S using synchrotron-based X-ray absorption near edge spectroscopy (XANES). We found that acetone dehydration and resin replacement in a 100% N_2 glovebox successfully preserved the speciation of Fe and Mn minerals within laminated sediments. However, acetone removed some sulfur species from sediments, and epoxies contained sulfur species, which challenged identification of native sulfur species. Results from this study will aid researchers who are interested in spatial analysis of oxygen sensitive sediments, soils, or microbial mats in choosing a preservation method.

Introduction

Persistent anoxia can develop in the bottom waters of deep lakes due to a lack of complete mixing, which minimizes sediment resuspension and bioturbation (Anderson et al. 1985). The sediments of such lakes often accumulate laminations that represent seasonal changes in the deposited components (i.e. varves), composed of organic material and/or mineralized biological organisms, detrital material, and chemically precipitated minerals (Anderson and Dean 1988). Lakes with laminated sediments can record climatic transitions, vegetation changes, changes in sediment transport, and atmospheric deposition patterns (O'Sullivan 1983). Laminated

sediments are also useful to study the formation, deposition, and diagenetic transformation of chemically precipitated minerals in aquatic sediments. The ability to constrain the formation, deposition, and diagenesis of chemical precipitates formed from redox-active elements within chemically stratified lakes offers a lens to interpret the origin of minerals in sediments deposited from redox-stratified marine basins in the past, particularly when such conditions no longer exist (Degens and Stoffers 1976). Such minerals are often composed of the most abundant redox-active elements in crustal materials (e.g. iron, manganese, and sulfur). However, a major challenge is the preservation of both primary sedimentary features such as laminations as well as primary mineralogy of minerals precipitated in the water column or sediments and/or under early sedimentary diagenesis, as these minerals may rapidly oxidize under ambient atmospheric conditions. This study focuses on best practices for preserving the redox state and mineralogy of material composed of Fe, Mn, and S in laminated sediments and particulate matter in the water column from a meromictic (i.e. permanently stratified) lake.

First described in 1958, freeze-coring is a method that preserves the structure of the sediment-water interface by freezing sediments onto the side of a wedge filled with dry ice and an organic solvent (e.g. isopropyl alcohol, butanol; Shapiro 1958). Variations on this method have been used to preserve laminated sediments for varve counting or dating (Saarnisto et al. 1977). More recently, this method has been used for successful bacterial community analysis using amplicon sequencing of the 16S rRNA gene (Harrison et al. 2015). Due to the low temperatures achieved, this method also holds promise to preserve redox-sensitive minerals under atmospheric oxygen if cores are maintained frozen such that oxidation reactions occur much more slowly than under ambient temperatures.

Preservation of sediment core structure for later spatial analysis can be accomplished through protocols that replace water with a solvent such as acetone, and then introduce epoxy to stabilize the sediments (Lamoureax 1994). The advantage of this technique is that thin sections of cast samples can be made to microscopically identify and count varves (Lotter and Lemcke 1999). It has also been used in an anoxic glovebox for the retention of oxygen-sensitive metals during washing/desalinization and fluid replacement (Jilbert et al., 2008).

The objective of this study is to assess sediment preparation and preservation techniques for lacustrine sediments with the goal of evaluating their utility for 1) maintaining the oxidation state and mineralogy of Fe, Mn, and S minerals, and 2) preserving spatial information, such as laminations. Samples of lake sediments and sediment trap material were chosen for this study, as both are useful to investigate the chemical precipitation of minerals in the water column or sediment porewaters, as well as early diagenetic transformation of minerals. The potential of different preservation techniques was evaluated with synchrotron-based XANES, which provides element-specific oxidation state information as well as mineralogical fingerprints.

Materials and Procedures

Sample Collection

Sediment cores and sediment trap samples were recovered from Brownie Lake in Minneapolis, Minnesota, U.S.A. Brownie Lake is a ferruginous and meromictic lake with relatively small surface area of 5 ha compared to its maximum depth of 14 m (Myrbo et al., 2011). It has been meromictic since 1925 after a canal connecting Brownie to Cedar Lake lowered its water level by several meters in 1914 (Swain et al., 1980). The onset of sediment laminations enriched in

iron and manganese within Brownie occurred after canal construction but prior to the transition to meromixis (Tracey et al., 1996).

Brownie Lake has a redoxcline at depth that varies seasonally from 3-5 m, which produces opposing gradients between dissolved oxygen and reduced chemical species (Lambrecht et al, 2018). The dissolved iron content exceeds 1 mM in the permanently anoxic monimolimnion, and dissolved manganese is in the range of tens of μM. Both dissolved iron and manganese are presumed to be predominantly in their more soluble, reduced (e.g. Fe^{2+} and Mn^{2+}) forms. Sulfate concentrations in the mixolimnion are seasonally variable with maxima in the epilimnion from 50-100 μM. Sulfate concentrations diminish with depth, which in combination with periodic detection of hydrogen sulfide below the redoxcline indicates vigorous biological sulfate reduction (Lambrecht et al., 2018). Five years of seasonal water chemistry data are available for Brownie Lake (Swanner et al. 2021).

Samples prepared and analyzed in this work are listed in **Table 1**.

Table 1. List of samples analyzed in this study, and the preparation steps compared.

Element	Sample Name	Sample and Preparation Type	Sample Depth	Sample Collection Date	Beamline	Analysis Date
Fe	BLI7	freeze core thin section	16 to 19 cm	Jan. 2018	13-IDE	Aug. 2019
Fe	BL18to20	bulk gravity core	18 to 20 cm	Oct. 2019	9-BM	Oct. 2020
Fe	BL11	grain mount particulate	11 m	Summer 2019	13-IDE	Aug. 2019
Fe	BLS10pt5	bulk particulates	10.5 m	Summer 2018	9-BM	Jul. 2020
Mn	BLI7	freeze core thin section	16 to 19 cm	Jan. 2018	13-IDE	Aug. 2019
Mn	BL18to20	bulk gravity core	18 to 20 cm	Oct. 2019	9-BM	Oct. 2020
S	BLII5	freeze core thin section	32 to 36.5 cm	Jan. 2018	13-IDE	Aug. 2019
S	BL28to30	bulk gravity core	28 to 30 cm	Oct. 2019	9-BM	Oct. 2020
S	BL28to30	grain mount gravity core	28 to 30 cm	Oct. 2019	13-IDE	Oct. 2020

Sediment Freeze core (BLI7 and BLII5)

A frozen core was extracted on January 12, 2018, at a water depth of 13 m using a stainless-steel ice corer rented from the National Lacustrine Core Facility at the University of Minnesota. The

procedure followed has been described in Harrison et al. (2015). Briefly, the corer was filled with a mixture of isopropyl alcohol and dry ice, which has a temperature of -78°C, and driven into the sediment on rods. After 20 minutes, the corer was returned to the surface and filled with lake water to slightly thaw the frozen sediment slabs on either side until they could be pried off (**Figure 1**). The core slabs were transported to the laboratory on dry ice and smoothed with a wood planar following steps outlined in Harrison et al. (2015), then cut into vertical strips 2-3 cm wide using a band saw. During handling, cores were maintained on dry ice, which has a temperature of -78.5°C. The frozen cores were shipped to Iowa State University on dry ice, where they were stored in a -80ºC freezer.

Sediment Gravity Core (BL18to20 and BL28to30)

A wet sediment core of about 30 cm was collected from a water depth of 13 m on October 4, 2019, with a National Lakes Assessment gravity corer from Aquatic Research Instruments. The core was immediately extruded into 2 cm increments inside of a N_2-filled disposable glove bag on the shore (**Figure 1**). Sediment increments were stored in 50 mL acid-washed glass media bottles flushed with N_2 and sealed with butyl rubber stoppers and aluminum crimps. The stoppered bottles were stored at 4°C.

Sediment traps (BL10pt5 and BL11)

Particulate matter within the water column of Brownie Lake was collected using sediment traps. The caps of 1L HDPE bottles were hollowed out to accommodate 4.5 cm diameter rigid tubes of about 50 cm long. The tubes were inserted into the hollowed caps and sealed with silicone glue. Once dry, the caps were screwed onto the 1L bottles to create a sediment trap (**Figure 1**). The trap was secured to rope attached to an anchor and buoy moored in the deep basin of Brownie Lake. The top of the sediment trap used in this study was located at a depth of 10.5 m below the

130 water surface. The trap was filled with water from the target depth using a van Dorn sampler
131 prior to trap deployment. The traps were left from May to September in 2018 and 2019 to collect
132 sedimenting material and chemically precipitated minerals from the water column. The deepest
133 sample collected in 2018 was from 10.5 m and from 11 m in 2019.
134 At the end of deployment, the sediment trap was pulled to near the water surface and the cap
135 with the tube was replaced with an intact cap while still underwater. The closed HDPE bottle
136 was immediately transferred into a N_2-filled glovebag on board the boat. Once the glovebag had
137 been purged with N_2, the contents of the 1L bottle were decanted into a 1L glass media bottle
138 and sealed with a butyl rubber stopper and cap. Samples were transported and stored at 4°C.
139
140 *Sample Preparation*
141 *Freeze core embedding and thin sectioning (BLI7 and BLII5)*
142 The workflow for embedding the freeze core and preparing thin sections is shown in **Figure 1**.
143 Aluminum trays were custom made to snuggly fit three sections to be embedded to maintain the
144 original core shape. The enclosing aluminum trays had pre-drilled holes in the bottom of the
145 trays to allow fluid exchange modeled after previous studies (e.g. Francus and Asikainen 2001;
146 Röhrig and Scharf 2006; Jilbert et al. 2008) The trays had about 20-25% open surface area as
147 holes, which allowed for sufficient fluid exchange. Work up until this point was done outside of
148 the 100% N_2 glovebox but samples were kept on dry ice when not being handled to prevent
149 thawing and oxidation. The still-frozen cores were then transferred into a 100% N_2 hard-sided
150 glovebox (Vacuum Atmospheres). The three aluminum trays were then placed in a disposable
151 aluminum pan. This pan was then placed into a Pyrex cooking pan with a snap lid for
152 embedding.

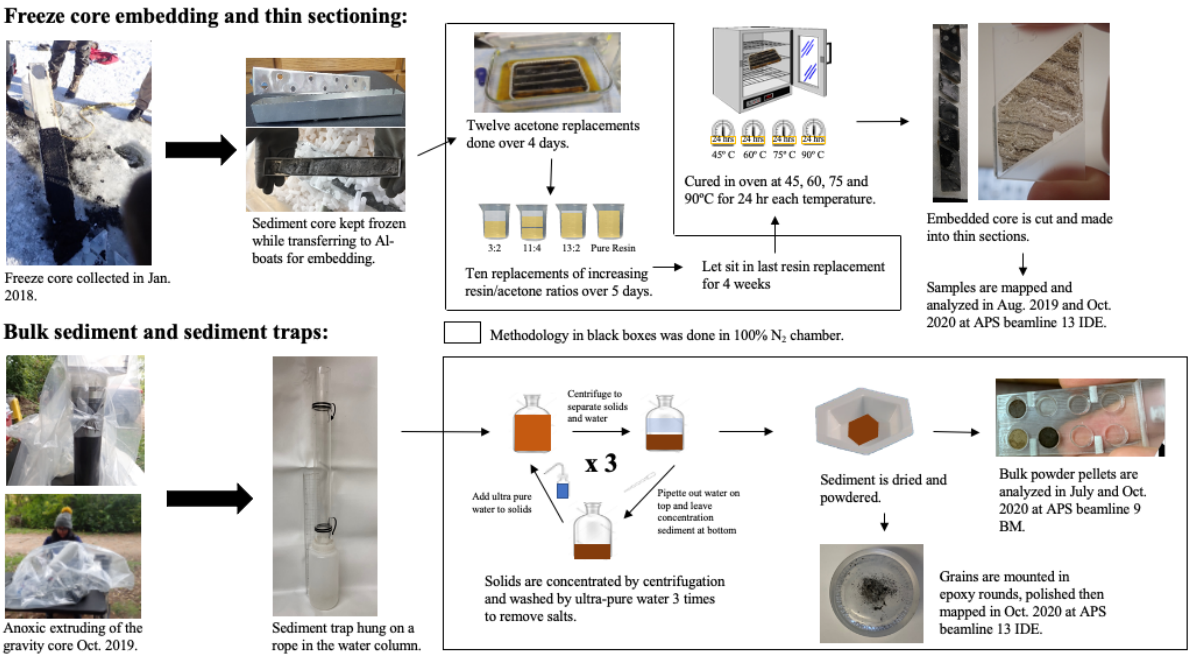

Figure 1: Schematic of sample collection, preparation, and analysis. The freeze core was embedded and thin sectioned for XRF mapping and microXANES. The gravity core and sediment trap material were washed and dried and used for bulk XANES and/or embedded as grain mounts for microXANES.

Dehydration of the samples was done via acetone replacements that began immediately once the samples were in the glovebox and before cores began to thaw. Beforehand, glass 1 L media bottles of acetone were made anoxic by bubbling with N_2 for 45 minutes under a fume hood. These bottles were sealed with butyl rubber stoppers and screw caps and brought into the glovebox. Anoxic acetone was slowly pipetted into the larger aluminum pan to fully submerge the still-frozen core sections. The pan was sealed with a tightly fitting and acetone-compatible snap cover between replacements. Replacements involved fully pipetting out the old acetone and replacing it with new anoxic acetone at 9 am, 12 pm, and 3 pm for four consecutive days for a total of 12 acetone replacements. Aside from the transfer of old and new acetone, the sediments were always fully submerged to preserve fragile lamination of the sediment.

168 Immediately following the 12 acetone exchanges, 10 increasing ratios of resin:acetone exchanges
169 began. Exchanges 1 through 3 had a resin:acetone ratio of 3:2, exchanges 4 and 5 had an 11:4
170 ratio, exchanges 6 and 7 had 13:2, and exchanges 8 through 10 were pure resin. The epoxy resin
171 was a 4-component mixture of Spurr's Resin consisting of Nonenyl Succinic Anhydride (NSA),
172 Cycloaliphatic Epoxide resin (ERL), Diglycidal Ether of Polypropyleneglycol (DER), and
173 Dimethylaminoethanol (DMAE) available from Electron Microscopy Sciences (**Table 2**). The
174 embedding procedure closely followed other embedding protocols (e.g. Jilbert, 2008, Grimm
175 1992, Lamoureux 1994, Pike and Kemp, 1996 and Lotter and Lemcke 1999). The four resin
176 components, ERL, NSA, DER, and DMAE made up 35.7%, 51.4%, 12.5%, and 0.4% of the
177 epoxy mixture, respectively. These components were freshy mixed gravimetrically in a plastic
178 beaker under a fume hood before each exchange. If bubbles could be seen in the resin, beakers
179 were put in a Polyvac vacuum impregnator (Presi GmbH) at 80 kPa for 15 minutes on the bench
180 to remove air bubbles as they could release oxygen into the glovebox. Instead of three vacuum
181 and evacuation cycles, the glovebox antechamber was deoxygenated by simultaneously
182 evacuating and adding gas, but with just a slight vacuum such that automatic gas injections kept
183 pace with the evacuation, ~2x per second. After 10 minutes, the epoxy was brought in with no
184 significant change to the glovebox oxygen levels (<1 ppm).

Table 2. Epoxy components used for embedding of sediments and sediment trap material.

Brand	Epoxy Name	Components	Part Number
Fluid replaced and thin sectioned freeze core (BLI7 and BLII5)			

Electron Microscopy Sciences	Spurr's Resin	Dimethylaminoethanol (DMAE)	13300
		ERL 4221	15004
		DER 736	13000
		Nonenyl Succinic Anhydride Modified (NSA)	19050
Grain mounts of sediment trap particulates (BL11)			
Epoxy Technologies	Epo-tek	Kit Part A	301
		Kit Part B	301
Grain mounts of sediment trap particulates and gravity-cored sediments (BL18to20, and BL28to30)			
Buehler	EpoxiCure 2	Resin	20-3430-064
		Hardener	20-3432-016
		Release Agent	20-8186-004

Once in the glovebox, the four-component resin mixture was mixed in a plastic beaker with measured anoxic acetone to create the appropriate resin/acetone mixture. In similar fashion to the acetone replacements, the increasing ratios of resin/acetone mixture were carefully pipetted in and out of the pan every 12 hours for a total of 10 exchanges over 5 days, again taking care to keep all sediment submerged. The leftover resin/acetone mixture was put into a plastic beaker, removed from the glovebox, and left in a fume hood to harden prior to disposal. After the final resin exchange, special care was taken to assure all material was fully submerged with the 4-component resin and the resin-covered sediments sat undisturbed to harden for 4 weeks in the glovebox. After 4 weeks, the glass pan containing the hardened sediments was sealed with the snap cover and removed from the glovebox and cured in an oven at temperatures of 45, 60, 75, 90ºC for 24 hours each for a total of 4 days.

Following the curing, the three Al-trays were separated by cutting the embedded block between each tray using a band saw, being careful to avoid cutting directly into the sediment and potentially expose it to oxygen. The embedded sediment cores were transported to TPS Enterprises for thin sectioning using no water during the cutting and polishing. The embedded

sediment core and subsequent thin sections were transported via sealed mylar bags with oxygen-removing packets contained in the bag.

Thin sections and sediment blocks were maintained in the 100% N_2 glovebox or N_2-filled jars for long-term storage. For transport to analytical facilities, the thin sections were heat sealed in mylar bags in the glovebox with oxygen-removing packets.

Bulk Sediment and Sediment traps (BL10pt5, BL11, BL18to20, and BL28to30)

Sediment trap waters were pipetted into 50 ml media bottles sealed with butyl rubber stoppers inside the glovebox and centrifuged outside the glovebox at 1700 rpm for 10 minutes to concentrate solids. Higher speeds were avoided to prevent glass bottles from breaking. The supernatant was removed using a pipette inside the glovebox, and more sample was added until all the sediment from a 1L trap was concentrated in the small bottle. To remove salts, both the sediment trap and gravity cored sediments were washed three times with anoxic 18.2 mΩ water, centrifuged, and the wash water was removed by pipette. Water was made anoxic by microwaving 1L in a glass media bottle to a near boil and then cooling under a N_2 stream and sealing with a butyl rubber stopper and screw cap before bringing it into the glovebox.

Sediment porewater was extracted with Rhizon samplers (Rhizosphere Research Products) with a pore size of 0.15 μm inside the glovebox (Islam 2022).

After washing or porewater extraction, the sediment or sediment trap material was dried inside the glovebox or under the vacuum in the antechamber. Once dried, sediments were pressed into 7 mm pellets and loaded onto custom sample holders from the beamline using carbon tape. Sample holders were then wrapped tightly in clingfilm with cardstock wedged between the sample holder and the top lid to minimize movement of the pellets during sample transport. Sample

holders were heat sealed in mylar bags inside the glovebox with oxygen-removing packets for transport to the synchrotron.

The sediment trap samples compared were from two different years and the collection depth differed by 0.5 m. The samples are comparable as the monimolimnion water chemistry conditions do not vary much from year to year (Lambrecht et al. 2018). Also, Mössbauer spectroscopy results indicate that Fe mineralogy of sediment traps does not vary significantly below the chemocline (Islam 2022).

Epoxy Grain Mounts of sediments and sediment traps (BL10pt5 and BL18to20)

To assess an additional epoxy preparation technique, the sediment trap sample (BL10pt5) and gravity cored sediment sample (BL18to20) were embedded in epoxy ring molds inside the glovebox using EpoTek for BL10pt5 and EpoxyCure™ 2 Resin and Hardener for the BL18to20. Washed and dried sediments were sprinkled onto the bottom of silicon holders for 1-inch (2.54 cm) ring molds (Presi GmbH or Buehler). The two epoxy components were mixed outside the glovebox and bubbles were removed in a Polyvac vacuum impregnator (Presi GmbH) at 80 kPa for 15 minutes on the bench. The degassed epoxy was then brought into the glovebox using simultaneous vacuum and degassing for 10 min to avoid disturbance of the epoxy with subsequent purge cycles. The epoxy was poured into rounds and left to cure for >24 hours inside the glovebox. Two different epoxies were used due to supply issues (**Table 2**).

After hardening, the sample surface of the epoxy grain mounts was polished inside the glovebox using a small Dremel tool with a flat-top attachment with sandpaper or polishing papers glued on the surface. Microgrit sandpaper was used to polish the grain mounts, starting with coarser sandpaper and ending with very fine-grained sandpaper. The five sandpaper grits used were 240,

320, 500, 600, 800 and 1000 on the Coated Abrasives Manufacturing Institute (CAMI) scale, with a higher number corresponding to a finger-grained sandpaper. The epoxy rounds were polished until the surface showed a clear cluster of sample material with even distribution for ease of analysis.

X-ray Absorption Spectroscopy (XAS)

Bulk analysis

Bulk sediment trap and gravity cored sediments were analyzed with XANES spectroscopy at the Fe, Mn, and S k-edges at beamline 9-BM at the Advanced Photon Source of Argonne National Laboratory. Samples were opened in a N_2-filled glovebag inside the hutch and transferred as quickly as possible into the helium-filled sample chamber. Samples were analyzed in fluorescence using a Vortex four element silicon drift detector. Energy was calibrated with an Fe foil and the E_0 set to 7112 eV, and a Mn foil with E_0 set to 6539 eV. Fifteen to twenty sulfur scans were collected and averaged for each bulk sample, and 3-4 scans were collected for iron, and 5-10 scans for manganese. Channels were summed and deadtime corrected at the beamline.

Microscale analysis

Embedded thin sections and grain mount samples were opened inside a glovebag (90% N_2, 10% H_2) at the laboratory of beamline 13-IDE at the Advanced Photon Source of Argonne National Laboratory and transferred in glass jars to the sample chamber, which was encased in a helium-purged bag. Individual areas of <1x1 mm were mapped using X-ray fluorescence (XRF) at 7200 eV for Fe and Mn and 2500 eV for sulfur on thin sections and grain mounts. Spots chosen for microXANES at the Fe, Mn, and S K-edges based on the XRF maps.

All analytical files (spectra and maps) as well as additional analytical data are publicly available and reusable (Swanner et al. 2022).

Data Analysis

Iron and Manganese

XANES spectra of bulk sediment measured at the Fe and Mn K-edges were averaged, background subtracted, and normalized by linear regression through the pre- and post-edge using SixPACK (Webb 2005). A principle component analysis was utilized to identify the distinct spectra ("end-members") from each mapped area (Mayhew et al. 2011; Swanner et al. 2019). End-member microXANES at either the Fe or Mn K-edge of the embedded thin sections were processed as individual files and averaged for each edge across all mapped areas to produce a "bulk" spectrum from microscale analyses. The resulting individual and averaged files of Mn and Fe were background subtracted and normalized using SixPACK. Pre-edge peak fitting was done in XAS Viewer (Version Larch 0.9.58, https://xraypy.github.io/xraylarch/). A baseline was fit to the pre-edge and initial edge jump region using a linear and Lorentzian model. One to two gaussian peaks were fit to the pre-edge peak.

Published reference spectra were used for comparisons for Fe (O'Day et al. 2004) and Mn (Manceau et al. 2012; Leven et al. 2018).

Sulfur

Sulfur XANES spectra were processed in Athena (Ravel and Newville 2005) by fitting a polynomial to the pre- and post-edge regions and normalizing the edge jump to 1.0. Peak fitting

using gaussian curves and arctangent functions was performed in the 2465 to 2485 eV region of the spectra to identify major components by their characteristic peak energies.

Assessment

We assessed if our modified methodology of embedding sediment cores and sediment trap particulates under oxygen-free conditions could successfully maintain the oxidation state and *in situ* mineralogy of Fe, Mn, and S within chemically precipitated minerals forming in a meromictic lake. To test this, the Fe, Mn, and S speciation from the embedded thin sections and embedded grain mount samples were compared to the non-embedded homogenized sediment trap and gravity-cored sediment analyzed in bulk from similar locations within Brownie Lake. Our assumption was that the bulk samples that were not embedded would best preserve both oxidation state and mineralogy because they were the least processed (e.g., due to acetone dehydration or potential chemical reaction with epoxy during the embedding process, or through oxygen exposure during thin section preparation and polishing). The ability to maintain both redox and spatial structure in preparation techniques would be advantageous relative to bulk analysis because it would allow for microscopic work, mapping, and identification of less abundant minerals.

To assess whether oxidation state of Fe was preserved we fit the pre-edge peaks of the bulk sample spectra and the averaged microXANES spectra from end-members of the mapped areas on the embedded thin section or grain mount of sediment trap particulates (**Figure 2**). For the sediment samples, the averaged spectral pre-edge peaks from BLI7 and BL18to20 were fit with two Gaussians each (**Table 3**). A t-test of the centroid positions resulted in a two-tailed p value of 0.4965. This indicates that there is no difference in the oxidation state of sediment samples prepared as thin sections to the bulk samples that were not embedded.

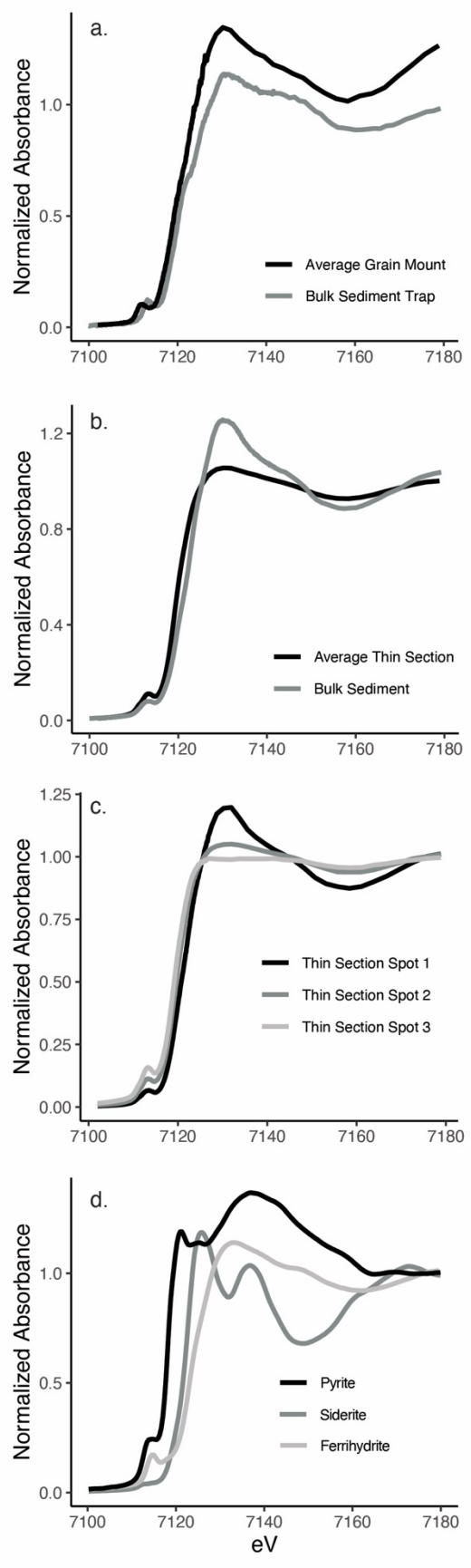
a.
Normalized Absorbance
1.0
0.5
0.0
Average Grain Mount
Bulk Sediment Trap
7100
7120
7140
7160
7180
b.
Normalized Absorbance
1.2
0.8
0.4
0.0
Average Thin Section
Bulk Sediment
7100
7120
7140
7160
7180
c.
Normalized Absorbance
1.25
1.00
0.75
0.50
0.25
0.00
Thin Section Spot 1
Thin Section Spot 2
Thin Section Spot 3
7100
7120
7140
7160
7180
d.
Normalized Absorbance
1.0
0.5
0.0
Pyrite
Siderite
Ferrihydrite
7100
7120
7140
7160
7180
eV

313

Figure 2: Iron XANES results. A. The average microXANES from end-member spectra on a grain mount of sediment trap samples and the bulk XANES of that sample. B. The average microXANES from end-member spectra on a thin section of sediments and the bulk XANES of that sample. C. End-member microXANES spectra from the thin sectioned sediment in B compared to D. the spectra of reference materials. The oxidation state of Fe in the pyrite (Fe-sulfide) and siderite (Fe-carbonate) standards is 2, while it is 3 in the ferrihydrite (Fe-oxide; O'Day et al. 2004).

The sediment trap sample pre-edge peak fits used only one Gaussian, as additional Gaussian peaks did not improve the χ^2. However, the centroid energies of the two sample types were separated by more than 1 eV, indicating that Fe in BL10pt5, the bulk sample, was more oxidized than in the embedded sample. This difference in oxidation state is likely a result of the targeting of Fe-rich particles for microXANES, which may have a slightly different speciation than particles in which iron is less concentrated than in oxides or sulfide. In lakes this could include clays with oxidized iron (Björnerås et al. 2021). Mössbauer analyses of the sediment trap samples from Brownie Lake indicated that about 40% of iron in sediment traps was present in Fe(II) and Fe(III) bearing clays (Islam 2022). These minerals may not have been targeted in microXANES of Fe-rich grains but would contribute substantially to the bulk Fe signal of sample BL10pt5. It is unlikely that acetone solubilized any iron minerals from the embedded sediments, as iron minerals are generally dissolved with acids rather than organic solvents (Poulton and Canfield 2005).

Table 3. Fe K-edge pre-edge characteristics and standard deviations for Brownie Lake samples.

Sample	Height	Position (eV)	FWHM (eV)	Area	Total Area	Centroid (eV)	χ^2
BLI7	0.056±0.000	7113.01±0.01	2.71±0.02	0.162±0.002	0.187±0.028	7112.74±0.07	1.74×10^{-5}
	0.013±0.000	7110.96±0.03	1.72±0.05	0.025±0.002			

BL18to20	0.032±0.006	7112.50±0.31	2.99±0.28	0.103±0.029	0.121±0.038	7112.68±0.02	$6.81x10^{-6}$
	0.008±0.010	7113.71±0.11	2.00±0.49	0.018±0.025			
BL11	0.055±0.002	7112.01±0.02	2.58±0.08	0.151±0.001	0.151±0.001	7112.01±0.02	$9.57x10^{-4}$
BL10pt5	0.068±0.001	7113.37±0.02	2.56±0.05	0.184±0.006	0.184±0.006	7113.37±0.02	$1.53x10^{-4}$

For Mn, the E^0 of the bulk averaged spectrum was 6546.07 eV and the average E^0 of the thin section end-member spectra was 6546.05 eV (**Figure 3**). This indicates that Mn is in the same oxidation state in embedded samples as in bulk sediment, as Mn^{2+} (Manceau et al. 2012). Slight differences in speciation may also reflect targeting of more Mn-enriched regions for microXANES as compared to bulk analysis. The end-member Mn XANES of the sediment sample had a similar pre-edge peak to Mn-carbonate and peak shapes like aqueous Mn^{2+} and lacked the energy shift characteristic of an oxide (**Figure 3c**). These results indicate that the oxidation state of both Fe and Mn was preserved in all samples during embedding and was likely Mn^{2+}.

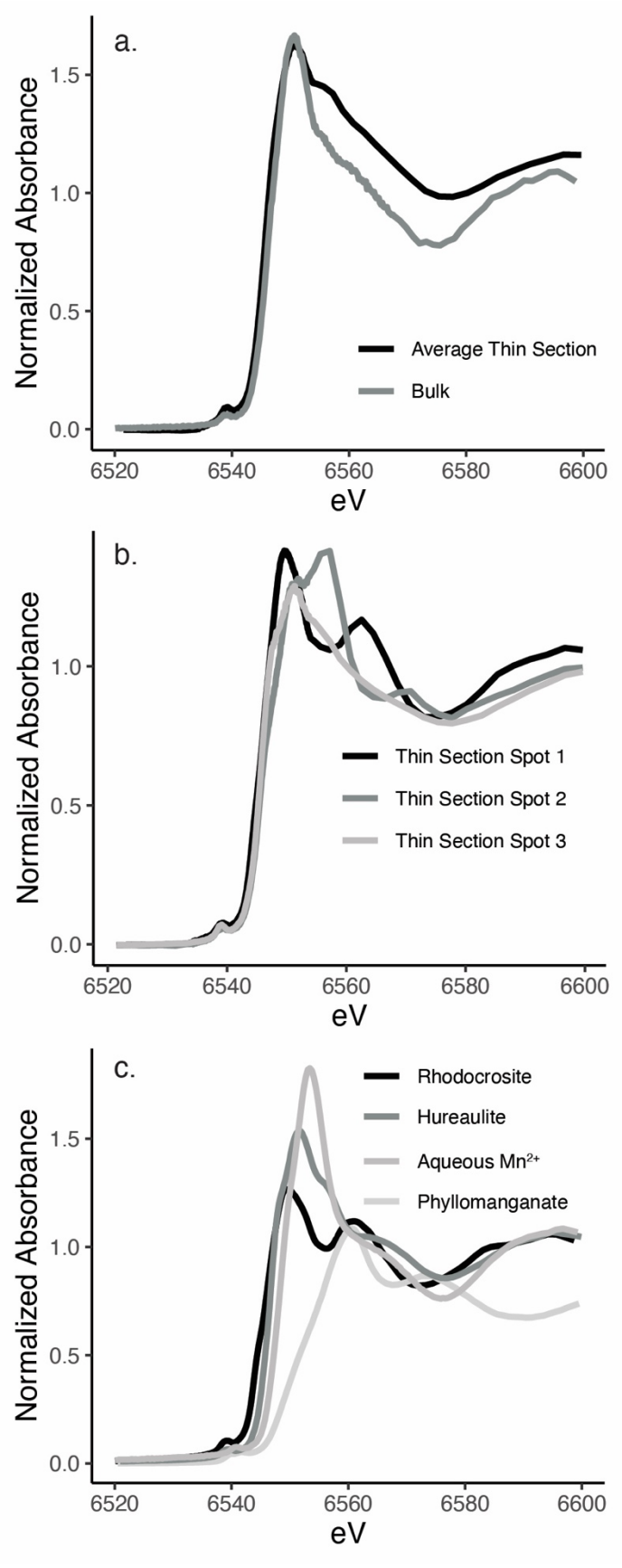
a.
Normalized Absorbance
1.5
1.0
0.5
0.0
6520
6540
6560
6580
6600
eV
Average Thin Section
Bulk
b.
Normalized Absorbance
1.0
0.5
0.0
6520
6540
6560
6580
6600
eV
Thin Section Spot 1
Thin Section Spot 2
Thin Section Spot 3
c.
Normalized Absorbance
1.5
1.0
0.5
0.0
6520
6540
6560
6580
6600
eV
Rhodocrosite
Hureaulite
Aqueous Mn2+
Phyllomanganate

347

Figure 3: Manganese XANES results. A. The average XANES from end-member spectra on a thin section of sediments and the bulk XANES of that sample. B. The average microXANES from end-member spectra of the thin sectioned sediment in A compared to spectra of reference materials. Manganese in rhodocrosite (Mn-carbonate) and hureaulite (Mn-phosphate) has an oxidation state of 2, while the average oxidation state of the phyllomanganate is 3.66 (Manceau et al. 2012).

To assess what S species were contained by the epoxies, XANES spectra were collected on an area of the thin section or grain mount with epoxy with no sample. Sulfur contamination in the Epo-Tek epoxy was not assessed in this study, but it has been used for microscale quantification of sample S with no problems (Reid et al. 2016). For thin sections, the Spurr's resin was fit with seven gaussian peaks, with the largest ones at 2472.82, 2477.55, and 2481.72 eV. The Buehler EpoxiCure 2 epoxy used in grain mounts of gravity-cored sediments *(BL28to30)* was fit with five gaussian peaks. It had two prominent S peaks near 2472 eV, a broad one at 2472.47 eV, and a narrower one at 2472.66 eV (**Figure 4**). A common S contaminant in both epoxies is likely a diphenyl disulfide (2472.7 eV), which has an oxidation state of S^{2-} (Almkvist et al. 2010). Such compounds increase the mechanical and thermal strength of epoxies (Tsai et al. 2020). The last contaminant peak in Spurr's resin is consistent with sulfonate or sulfate ester (Almkvist et al. 2010), which can be components of epoxies.

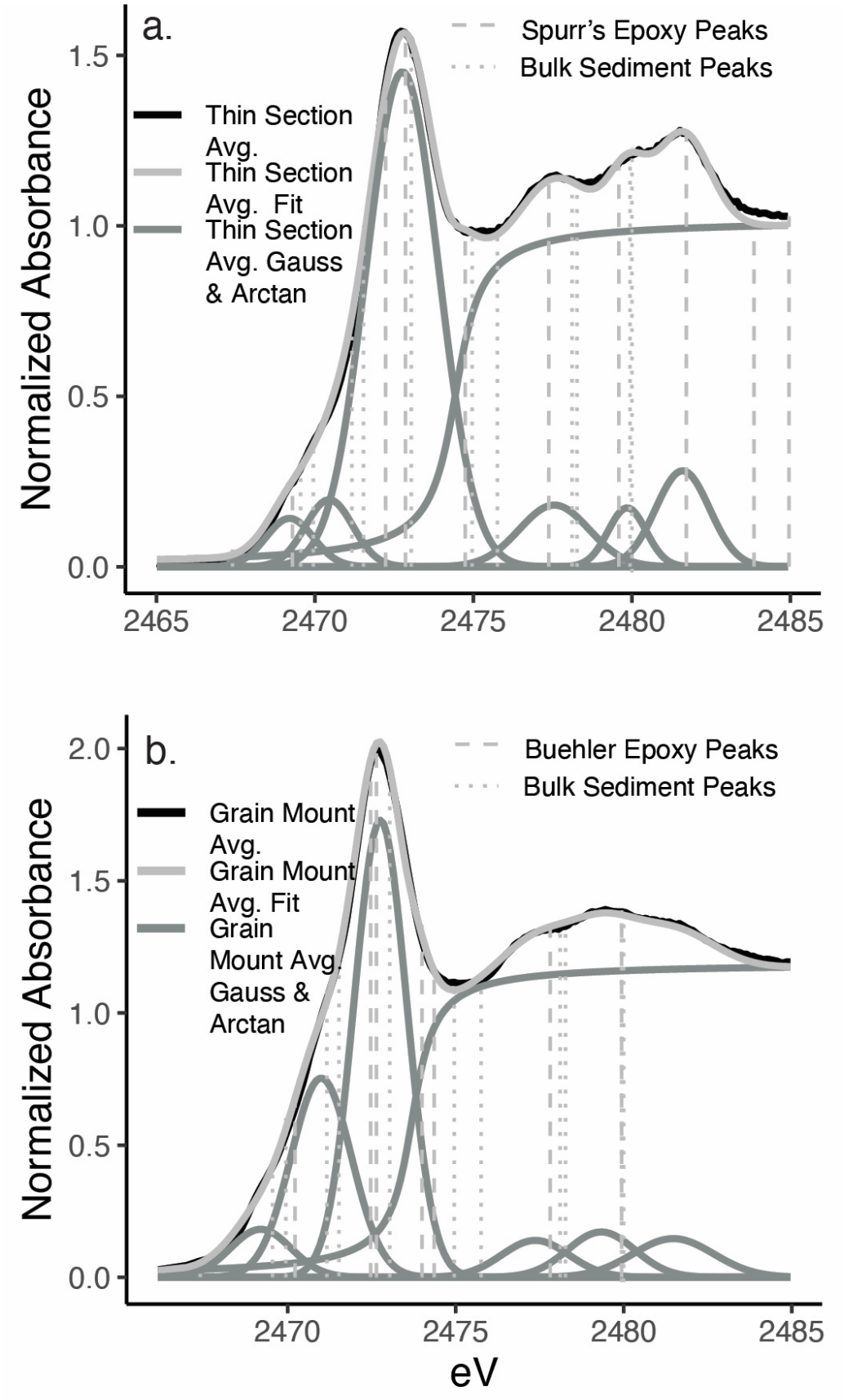
a.
Spurr's Epoxy Peaks
Bulk Sediment Peaks
Thin Section Avg.
Thin Section Avg. Fit
Thin Section Avg. Gauss & Arctan
Normalized Absorbance
1.5
1.0
0.5
0.0
2465
2470
2475
2480
2485
b.
Buehler Epoxy Peaks
Bulk Sediment Peaks
Grain Mount Avg.
Grain Mount Avg. Fit
Grain Mount Avg. Gauss & Arctan
Normalized Absorbance
2.0
1.5
1.0
0.5
0.0
2470
2475
2480
2485
eV

367

Figure 4: Sulfur XANES results. A. The averaged microXANES of the thin section end-members. Gaussian peaks and an arctangent are used to produce the fit. Peak energies of Gaussian functions used to fit the Spurr's resin used for embedding and the same sample analyzed in bulk with no preparation are plotted as vertical dashed and dotted lines. B. The averaged signal from averaged microXANES of the grain mount endmembers of gravity cored sediment. Gaussian peaks and an arctangent are used to produce the fit. Peak energies of Gaussian functions used to fit the Buehler Epoxicure resin used for embedding and the same sample analyzed in bulk with no preparation are plotted as vertical dashed and dotted lines.

The average spectra of endmember microXANES of the thin section was fit with six Gaussian peaks (**Figure 4a**). Four of these are attributable to sulfur from the Spurr's resin (2469.2, 2472.76, 2477.5 and 2481.6 eV). The remaining peaks (2470.45, 2479.85 eV) are attributable to an inorganic monosulfide, likely FeS, which has two peaks near these energies (Bostick et al. 2005; Swanner et al. 2019). Several peaks from 2473 through 2475 in the bulk spectrum may represent pyrite, elemental S, or organic disulfides/thiols (Bostick et al. 2005; Almkvist et al. 2010). These are absent in the thin section. Elemental S and some organic S may have been solubilized during repeated acetone washes. There is no inorganic sulfate peak in the thin section, which would be expected upon FeS oxidation (Burton et al. 2009). This suggests the S did not become oxidized during thin section preparation. However, a peak at 2467.4 eV is present in the bulk sample but absent in the thin section. This peak is not readily identifiable, but likely represents some reduced phase, which may not have been stable during preparation, either due to solubilization with acetone or reaction with epoxy. Iron sulfides are usually only solubilized under acidic conditions (Poulton et al. 2004). Another possibility is that the organic S

391 species were dispersed at low abundance within the sample and were not analyzed by
392 microXANES because they did not appear as S enriched particles in XRF mapping.
393 The grain mount sediment sample shared only one of the seven S peaks with the Buehler
394 Epoxicure 2, at 2472.64 eV. The grain mount samples are thicker than the 30 micron thin
395 sections, which may expose the sample more thoroughly for analysis due to less epoxy
396 permeation, but suffers from greater self-absorption effects. The grain mount shared a peak at
397 2469.55 eV with the bulk sediment, and also had a peak at 2471 eV, likely iron monosulfides,
398 which have been detectable in grain mounts before (Swanner et al. 2019). The grain mount had a
399 peak at 2481.24 eV, which was not detected in the bulk or epoxy, but could indicate sample
400 oxidation. Two other peaks between 2475 and 2480 eV were not present in the bulk sample,
401 which could indicate a reaction between organic S in the sample and the epoxy. The 2467.4 eV
402 peak from the bulk sample was also absent in the grain mount, suggesting it is not stable for
403 either type of embedding method.
404

405 **Discussion**

406 These results indicate that preservation by freezing or maintenance of oxygen-free conditions
407 and embedding in an anoxic chamber was sufficient to prevent oxidation of Fe and Mn minerals.
408 Keeping the core frozen during the initial preparation was unique to this study as other protocols
409 transferred sediment into the Al-trays using soft or unconsolidated sediment and pushing Al-
410 trays into an ambient temperature sediment core (Francus and Asikainen 2001; Röhrig and
411 Scharf 2006; Jilbert et al. 2008).
412 The ability to perform XRF and microXANES on discrete micron-scale area of embedded thin
413 sections was a strength of this technique for Fe minerals, as minerals that may be in low overall

414 abundance but were relatively enriched in Fe, such as Fe-sulfides, were not identifiable in the
415 bulk XANES spectra. This was less apparent for Mn, and the good agreement between bulk and
416 microXANES likely reflects the lower amounts of Mn in the samples as compared to Fe, such
417 that all Mn minerals were detected.
418 The embedding protocols had a major limitation for S, which was the presence S contaminants in
419 epoxy. This may be mitigated with the use of a S-free epoxy (Swanner et al. 2019). Another
420 limitation was that dehydration of samples with acetone may have removed elemental S and/or
421 organic S species. If spatially resolved analysis of S species is desired, embedding particles
422 directly vs. after acetone dehydration is preferable. However, peaks may have shifted in the grain
423 mounts from the original sample and are suggestive of a reaction between organic S species and
424 epoxies. A final limitation was that S in less concentrated forms such as organic material are
425 well-dispersed in samples and may be hard to target from XRF maps, which tend to highlight S-
426 enriched areas for further analysis. A benefit of the embedding was that Fe-sulfide minerals that
427 were in low abundance and not easily discernable from the bulk XANES were visible with XRF.
428 Embedding of laminated sediments also provides an alternative to manually separating distinct
429 laminations for bulk analysis (Bostick et al. 2005).
430 The methodology described here is time-consuming, expensive, and requires specialty
431 equipment. Freeze coring requires constructing or renting specialty equipment, handling of
432 hazardous materials in the field, and maintaining samples on dry ice or in a -80°C freezer.
433 Planing and cutting the frozen cores required specialty tools and took training as frozen cores
434 were brittle. Custom aluminum holders had to be fabricated for each core section by a machinist
435 to keep cores intact. The embedding procedure required a schedule of exchanges and large
436 quantities of acetone and epoxy. A hard-sided glovebox was required, as the material used in

soft-sided glovebox walls would react with acetone. Charcoal filters were employed in-line on the catalyst fan to remove acetone from the glovebox, and prior to venting the glovebox acetone to the room. The glovebox therefore required a ventilated space. Despite these measures, one tank of N_2 was pumped through the glovebox at the end of the procedure to purge acetone vapors from the box, which were evident by the smell of the vented air. The pump on the glovebox required maintenance for O-rings and pump oil after this procedure to mitigate damage from acetone.

It is recommended to have a custom fit of aluminum boats to sediment cores, as once they thaw can become quite 'mushy' and risk losing their spatial information. Sediment cores were frozen upon insertion into Al-boats unlike previous methodologies, and therefore the cores did not take up the full boat capacity due to irregularities (see Figure 1). If tne procedure for embedding involves the "cheese cutter" style of pushing Al-foil trays into unfrozen sediment modeled by other studies, it should be performed under anoxic conditions. We found our method had successful fluid flow during replacements and embedding stages with only ~20-25% of open surface are via holes at the bottom of the aluminum trays containing the sediment cores rather than the previously recommended 50%. Acetone replacements should begin as the core begins to thaw otherwise spatial information could be lost.

Some procedural limitations were that acetone leaked or wicked out of the doubly and triply stacked Al pans into the glass pan. During acetone dehydration this was mitigatable by keeping sufficient acetone in the pan to account for this wicking action and maintain the liquid level. However, once resin was used, resin also leaked out of the Al pans into the glass pan. This effectively hardened the Al pan to the glass pan upon drying, making it difficult to extract the embedded sections for thin sectioning. It could help to change to a fresh glass pan periodically to

prevent hardening, especially before curing, or to line the glass pan with aluminum foil before curing.

The fundamental flaw of the embedding methodology for sulfur is in the presence of sulfur contaminants. The Epotek 301 A/B epoxy does not contain sulfur (Reid et al. 2016), while the Buehler Epoxicure 2 and Spurr's resin do. Araldite 2020 A/B epoxy was used for grain mounts of iron sulfides in a previous study and did not have sulfur contamination (Swanner et al. 2019). However, this epoxy has limited distribution, for instance, it is not available in the United States. Epotek comes in one pound packaging, but to avoid a small order surcharge, five pounds must be ordered. This means that Epotek epoxy is only a good option for large embedding projects, as the epoxy also expires within 1-2 years of purchase. This presents a limitation of finding a reliable supplier of a sulfur-free epoxy.

The other problem with Epotek 301 A/B and Araldite 2020 A/B is that they have not been used with acetone dehydration and it is unclear if these S-free epoxies would be amenable to embedding sediment cores. When asked, Epoxy Technologies would not provide information about the miscibility of Epotek 301 A/B with acetone or ethanol. Another issue is that the S-free epoxies are two component epoxies, with one component being the hardener, and they harden relatively quickly (hours to days) after being mixed. In this regard, the temperature curing Spurr's resin is preferable for embedding sediment cores as it can move through the sediment fully as a liquid before hardening. Further experimental work would be required to test the suitability of these S-free epoxies for embedding sediment cores.

The analytical procedures used here were performed at a national lab and time was awarded competitively from a proposal. XAS is just one analytical possibility, and these samples may also be amenable to other techniques. Despite the costs in time and money, the embedding techniques

did allow for spatially resolved speciation of Fe, Mn, and S. Depending on the end user's needs, this methodology could be further adapted to the equipment and resources available at the home institution.

Application

The literature addressing laminated sediments as paleoclimate and palaeoecological archives is the source of the coring and embedding techniques that form the basis for the methods described in this paper (Saarnisto et al. 1977; Lotter and Lemcke 1999). As laminated sediments are deposited under anoxic conditions, they can also contain information about climatic or water chemistry transitions within the minerals that precipitate within the water column and deposit to sediments, or within the sediments themselves. Such minerals often contain the most abundant rock-forming and redox-active elements Fe, Mn, and S. While previous work has documented the utility of embedding sediment cores under anoxic conditions in a glovebox to preserve elemental abundances (Jilbert et al. 2008), our work specifically addresses the potential for such an embedding approach to retain the original oxidation state and mineralogy of the major redox-active elements Fe, Mn, and S. We demonstrate that such an approach has utility for preserving the spatial information of oxygen-sensitive samples that are often homogenized for redox speciation analysis (Zeng et al. 2013; Herndon et al. 2018).

While we demonstrate the application of the described embedding techniques on laminated lake sediments, the methodology could also be applied to other sedimentary material when preserving the oxidation state, elemental speciation, mineralogy, and spatial arrangement of soft sediment is required. Such studies are likely engaged in linking the inventory of redox-active elements and minerals to the overlying water chemistry in the case of lacustrine and marine sediment.

Laminations also occur in unlithified marine sediment cores and can inform changes in circulation or ventilation of the overlying water. Wetlands are biogeochemical hotspots and sediments and can contain multiple redox species of Fe, Mn or S (Zeng et al. 2013). Although not laminated, wetland sediments could still record changing conditions through time. Other types of material could include soils or unconsolidated sediments, particularly in the saturated to vadose zone transition, that are expected to contain horizons that record redox fluctuations (Marafatto et al. 2021). Microbial mats are relatively organic-rich, but can also contain redox zonation (Engel et al. 2007), and may be amenable to embedding (Iniesto et al. 2015).

Acknowledgements

Jessica Heck, Kristina Brady Shannon, Ryan O'Grady, Amy Myrbo of LacCore assisted with handling of the freeze core. Sergei Katsev, Moji Fakhraee, and Nick Lambrecht helped to collect the freeze core, and Zackry Stevenson helped to collect the gravity core. Chad Wittkop helped with the freeze core and sediment traps. Beamline scientists Matthew Newville and Antonio Lanzirotti at 13IDE and Tianpin Wu and George Sterbinsky at 9BM assisted with data collection and analysis at the Advanced Photon Source.

This work was supported by National Science Foundation (NSF) awards to Swanner (1660691, 1944946) and an American Chemical Society Petroleum Research Fund award to Swanner (59933-DNI2). Ledesma was also supported by a Dean's High Impact Award from the College of Liberal Arts & Sciences at Iowa State University.

Data Availability Statement

Data used in this study is available in a public repository. Swanner, E. D., R. Islam, G. Ledesma, C. Wittkop, S. Akam, E. Eitel, S. Katsev, B. Johnson, S. Poulton, and A. Bray. 2022. Geochemical data from sediments and porewaters from ferruginous and meromictic Brownie Lake, Minnesota, U.S.A. Environmental Data Initiative. doi:10.6073/pasta/68b50baa0a767ab33f2b7dd91948036e

References

Almkvist, G., K. Boye, and I. Persson. 2010. K-edge XANES analysis of sulfur compounds: An investigation of the relative intensities using internal calibration. J. Synchrotron Radiat. **17**: 683–688. doi:10.1107/S0909049510022946

Anderson, R. Y., and W. E. Dean. 1988. Lacustrine varve formation through time. Palaeogeogr. Palaeoclimatol. Palaeoecol. **62**: 215–235. doi:10.1016/0031-0182(88)90055-7

Anderson, R. Y., W. E. Dean, P. Bradbury, and D. Love. 1985. Meromictic Lakes and Varved Lake Sediments in North America.

Björnerås, C., P. Persson, G. A. Weyhenmeyer, D. Hammarlund, and E. S. Kritzberg. 2021. The lake as an iron sink - new insights on the role of iron speciation. Chem. Geol. **584**. doi:10.1016/j.chemgeo.2021.120529

Bostick, B. C., K. M. Theissen, R. B. Dunbar, and M. A. Vairavamurthy. 2005. Record of redox status in laminated sediments from Lake Titicaca: A sulfur K-edge X-ray absorption near edge structure (XANES) study. Chem. Geol. **219**: 163–174. doi:http://dx.doi.org/10.1016/j.chemgeo.2005.02.004

Burton, E. D., R. T. Bush, L. A. Sullivan, and others. 2009. Iron-monosulfide oxidation in natural sediments: Resolving microbially mediated S transformations using XANES, electron microscopy, and selective extractions. Environ. Sci. Technol. **43**: 3128–3134. doi:10.1021/es8036548

Degens, E. T., and P. Stoffers. 1976. Stratified waters as a key to the past. Nature **263**: 22–27. doi:10.1038/263022a0

Engel, A. S., H. Lichtenberg, A. Prange, and J. Hormes. 2007. Speciation of sulfur from filamentous microbial mats from sulfidic cave springs using X-ray absorption near-edge spectroscopy. FEMS Microbiol. Lett. **269**: 54–62. doi:10.1111/j.1574-6968.2006.00600.x

Francus, P., and C. A. Asikainen. 2001. Sub-sampling unconsolidated sediments: A solution for the preparation of undistrubed thin-sections from clay-rich sediments. J. Paleolimnol. **26**: 323–326. doi:10.1023/A

Harrison, B. K., A. Myrbo, B. E. Flood, and J. V Bailey. 2015. Identification of subannual patterns in microbial community signatures from individual sedimentary laminae using a freeze-coring approach. Limnol. Ocean. **61**: 735–747.

Herndon, E. M., J. R. Havig, D. M. Singer, M. L. McCormick, and L. R. Kump. 2018.

565 Manganese and iron geochemistry in sediments underlying the redox-stratified Fayetteville
566 Green Lake. Geochim. Cosmochim. Acta **231**: 50–63.
567 doi:https://doi.org/10.1016/j.gca.2018.04.013
568 Iniesto, M., N. Zeyen, A. I. López-Archilla, S. Bernard, Á. D. Buscalioni, M. C. Guerrero, and
569 K. Benzerara. 2015. Preservation in microbial mats: Mineralization by a talc-like phase of a
570 fish embedded in a microbial sarcophagus. Front. Earth Sci. **3**: 1–13.
571 doi:10.3389/feart.2015.00051
572 Islam, R. 2022. Investigating the Formation Mechanisms of Sedimentary Pyrite under Anoxic &
573 Ferruginous Conditions. Iowa State University.
574 Jilbert, T., G. de Lange, and G. J. Reichart. 2008. Fluid displaced resin embedding of laminated
575 sediments: preserving trace metals for high-resolution paleoclimate investigations. Limnol.
576 Ocean. Methods **6**: 16–22. doi:10.4319/lom.2008.6.16
577 Lambrecht, N. L., C. Wittkop, S. Katsev, M. Fakhraee, and E. D. Swanner. 2018. Geochemical
578 characterization of two ferruginous meromictic lakes in the Upper Midwest, U. S. A. J.
579 Geophys. Res. Biogeosciences **123**: 3403–3422. doi:10.1029/2018JG004587
580 Leven, A., D. Vlassopoulos, M. Kanematsu, J. Goin, and P. A. O'Day. 2018. Characterization of
581 manganese oxide amendments for in situ remediation of mercury-contaminated sediments.
582 Environ. Sci. Process. Impacts **20**: 1761–1773. doi:10.1039/c7em00576h
583 Lotter, A. F., and G. Lemcke. 1999. Methods for preparing and counting biochemical varves.
584 Boreas **28**: 243–252. doi:10.1111/j.1502-3885.1999.tb00218.x
585 Manceau, A., M. A. Marcus, and S. Grangeon. 2012. Determination of Mn valence states in
586 mixed-valent manganates by XANES spectroscopy. Am. Mineral. **97**: 816–827.
587 doi:10.2138/am.2012.3903
588 Marafatto, F. F., R. Dähn, D. Grolimund, J. Göttlicher, and A. Voegelin. 2021. Thallium sorption
589 by soil manganese oxides: Insights from synchrotron X-ray micro-analyses on a naturally
590 thallium-rich soil. Geochim. Cosmochim. Acta **302**: 193–208.
591 doi:10.1016/j.gca.2021.03.011
592 Mayhew, L. E., S. M. Webb, and A. S. Templeton. 2011. Microscale Imaging and Identification
593 of Fe Speciation and Distribution during Fluid-Mineral Reactions under Highly Reducing
594 Conditions. Environ. Sci. Technol. **45**: 4468–4474. doi:10.1021/es104292n
595 O'Day, P. A., N. Rivera Jr., R. Root, and S. A. Carroll. 2004. X-ray absorption spectroscopic
596 study of Fe reference compounds for the analysis of natural sediments. Am. Mineral. **89**:
597 572–585.
598 O'Sullivan, P. E. 1983. Annually-laminated lake sediments and the study of Quaternary
599 environmental changes — a review. Quat. Sci. Rev. **1**: 245–313.
600 doi:https://doi.org/10.1016/0277-3791(83)90008-2
601 Poulton, S. W., and D. E. Canfield. 2005. Development of a sequential extraction procedure for
602 iron: implications for iron partitioning in continentally derived particulates. Chem. Geol.
603 **214**: 209–221.
604 Poulton, S. W., M. D. Krom, and R. Raiswell. 2004. A revised scheme for the reactivity of iron
605 (oxyhydr)oxide minerals towards dissolved sulfide. Geochim. Cosmochim. Acta **68**: 3703–
606 3715. doi:10.1016/j.gca.2004.03.012
607 Ravel, B., and M. Newville. 2005. ATHENA, ARTEMIS, HEPHAESTUS: Data analysis for X-
608 ray absorption spectroscopy using IFEFFIT. J. Synchrotron Radiat. **12**: 537–541.
609 doi:10.1107/S0909049505012719
610 Reid, N., T. C. Robson, B. Radcliffe, and M. Verrall. 2016. Excessive sulphur accumulation and

611 ionic storage behaviour identified in species of Acacia (Leguminosae: Mimosoideae). Ann.
612 Bot. **117**: 653–666. doi:10.1093/aob/mcw009
613 Röhrig, R., and B. W. Scharf. 2006. An alternative embedding method for thin section
614 preparation of lake sediments. J. Paleolimnol. **35**: 207–209. doi:10.1007/s10933-005-2316-
615 5
616 Saarnisto, M., P. Huttunen, and K. Tolonen. 1977. Annual lamination of sediments in Lake
617 Lovojärvi, southern Finland, during the past 600 years. Ann. Bot. Fenn. **14**: 35–45.
618 Shapiro, J. 1958. The core-freezer--A new sampler for lake sediments. Ecology **39**: 758.
619 doi:10.2307/1931618
620 Swanner, E. D. ., S. M. Webb, and A. Kappler. 2019. Fate of cobalt and nickel in mackinawite
621 during diagenetic pyrite formation. Am. Mineral. **104**: 917–928. doi:10.2138/am-2019-6834
622 Swanner, E. D., R. Islam, G. Ledesma, and others. 2022. Geochemical data from sediments and
623 porewaters from ferruginous and meromictic Brownie Lake, Minnesota, U.S.A. Environ.
624 Data Initiat. doi:10.6073/pasta/68b50baa0a767ab33f2b7dd91948036e
625 Swanner, E. D., N. Lambrecht, C. Wittkop, S. Katsev, G. Ledesma, and T. Leung. 2021. Water
626 properties of Brownie Lake, MN and Canyon Lake, MI from 2015-
627 2019.doi:10.6073/PASTA/4EAF698B4EFBAF793B83D95F464D1672
628 Tsai, H. Y., Y. Nakamura, T. Fujita, and M. Naito. 2020. Strengthening epoxy adhesives at
629 elevated temperatures based on dynamic disulfide bonds. Mater. Adv. **1**: 3182–3188.
630 doi:10.1039/d0ma00714e
631 Webb, S. M. 2005. SIXpack: a graphical user interface for XAS analysis using IFEFFIT. Phys.
632 Scr. **2005**: 1011. doi:10.1238/Physica.Topical.115a01011
633 Zeng, T., W. A. Arnold, and B. M. Toner. 2013. Microscale Characterization of Sulfur
634 Speciation in Lake Sediments. Environ. Sci. Technol. **47**: 1287–1296.
635 doi:10.1021/es303914q
636